

Photodissociation and Photoionisation Dynamics and the Dissociation Energy of Niobium Oxide, NbO, Investigated using Velocity Map Imaging

Hansjochen Köckert, Alexander S. Gentleman, Jack Pickering, and Stuart R Mackenzie*

Department of Chemistry, Physical and Theoretical Chemistry Laboratory, South Parks
Road, Oxford, OX1 3QZ, United Kingdom

Supporting Information

KEYWORDS: velocity map imaging, metal oxide, dissociation energy, photodissociation,
photoionisation

Table of Contents

SI. Calibration of the OPO and Dye Lasers	3
SII. Velocity-Map Imaging of Photoelectrons	5
<i>A. Velocity calibration for imaging of photoelectrons</i>	5
<i>B. Photoionization of vanadium atoms</i>	8
SIII. References.....	11

SI. Calibration of the OPO and Dye Lasers

The output wavelengths of both the OPO and dye lasers were scanned over the $f^4F_J \leftarrow a^4F_J$ two-photon transition of neutral vanadium atoms in the molecular beam, prepared from laser ablation of a vanadium disc (Goodfellow, 99.98%). The V^+ yield is recorded as the (2+1)-REMPI spectrum with the OPO and dye laser, and the spectra are shown in Figure S1(a) on the top and bottom, respectively. The (2+1)-REMPI transition is schematically shown in Figure S1(b). Three photons in the green part of the spectrum are required to overcome the ionization potential of the vanadium atom at 54410 cm^{-1} [1] via the f^4F_J state manifold.

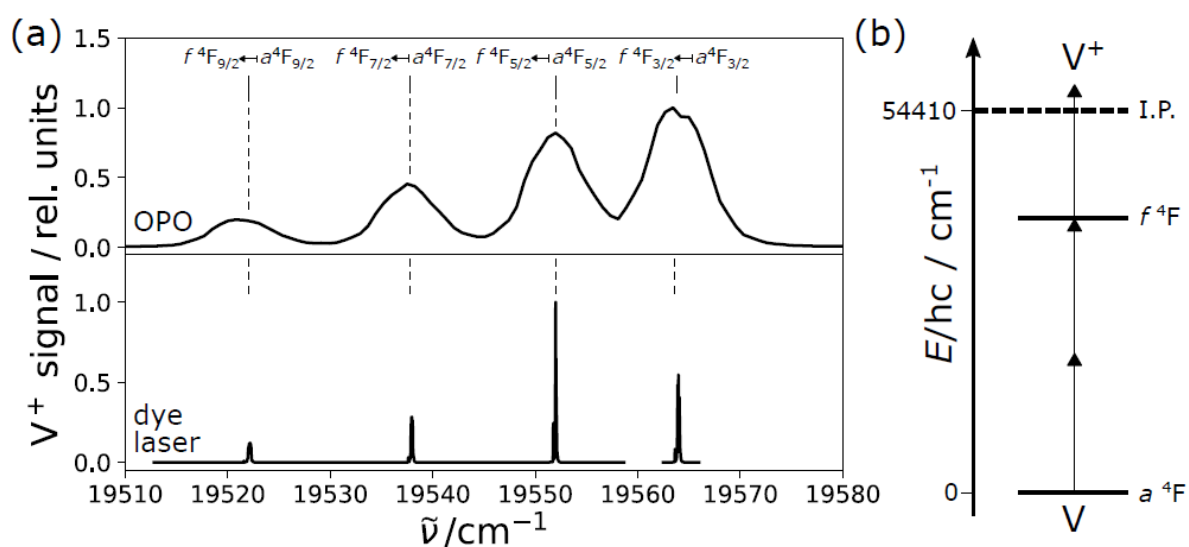


Figure S1. (a) (2+1)-REMPI spectrum of atomic vanadium, recorded as the V^+ ion signal for different wavenumbers of an optical parametric oscillator (top) and dye laser (bottom). In this spectral region, vanadium atoms are ionized in a three-photon transition as shown in (b). The photon energy of the ionization laser is resonant with the $f^4F_J \leftarrow a^4F_J$ two-photon transition from the ground state. A third photon is used to overcome the ionization potential (IP), from the f -state.

The (2+1)-REMPI spectrum of atomic vanadium is compared to known energy levels, E_V , of the a^4F_J ground state and f^4F_J -state manifold from Reference [2] and [3], which are listed in Table S1. Four transitions for $\Delta J = 0$ are observed in the REMPI spectrum in Figure S1, and in the following data analysis the wavelength of OPO and dye laser is corrected so that the observed lines match the tabulated values of the vanadium energy levels. The observed peak-width is consistent with the linewidths of the OPO ($< 6 \text{ cm}^{-1}$), and dye laser (0.08 cm^{-1}).

J	$E_V(a^4F_J) / \text{cm}^{-1}$	$E_V(f^4F_J) / \text{cm}^{-1}$
3/2	0.000	39127.228
5/2	137.383	39241.384
7/2	323.432	39398.893
9/2	552.955	39596.988

Table S1. Energy levels of the a^4F_J and f^4F_J manifold for $J = 3/2, 5/2, 7/2, 9/2$ for the vanadium atom. Values taken from References [2] and [3].

SII. Velocity-Map Imaging of Photoelectrons

The photoionization of niobium oxide and niobium atoms produces both ions and electrons. In the first velocity-map imaging studies, Eppink and Parker [4] showed that both ions and electrons can be recorded in a velocity-map imaging spectrometer by changing the polarity of the velocity-mapping field. While past experiments on our present spectrometer were solely focussed on the study of fragment ions, this is the first velocity-map imaging experiment detecting photoelectrons in our set-up. The kinetic energy and angular distribution of the detected electrons gives insight into the orbital the electron is emitted from, and on the electronic structure of the product ion.

One challenge in velocity-map imaging of photoelectrons is the low mass and, thus, small momentum of low kinetic energy electrons. Because electrons are at least three orders of magnitude lighter than ion products, their trajectories in the velocity-map imaging spectrometer are more easily perturbed by electric and magnetic fields than those of ions. These fields can originate from equipment inside and outside the experiment. Initially distorted velocity-map images have been greatly improved by identifying and eliminating sources of such fields in this experimental set-up. In the following, the velocity calibration of the spectrometer for photoelectrons is described and initial experiments imaging photoelectrons from the ionization of vanadium atoms are presented.

A. Velocity calibration for imaging of photoelectrons

Due to the large mass difference between ions and electrons, the magnification factor, N_{ele} , for velocity-map imaging of photoelectrons was redetermined simulating the electron trajectories in a model of the spectrometer using the SIMION software package [5]. To this purpose,

trajectories of ten groups of 1000 electrons with kinetic energies ranging from 0.5 eV to 5.0 eV are simulated for an extraction potential of 5000 V. Thus, a simulated velocity-map image of electrons in the model spectrometer was produced and is shown in Figure S2. The electron time-of-flight inside the spectrometer, $t_{\text{ele}} = 11.9$ ns, was also retrieved from the simulation. The simulated velocity-map image in Figure S2 is reconstructed using the pBASEX algorithm [6].

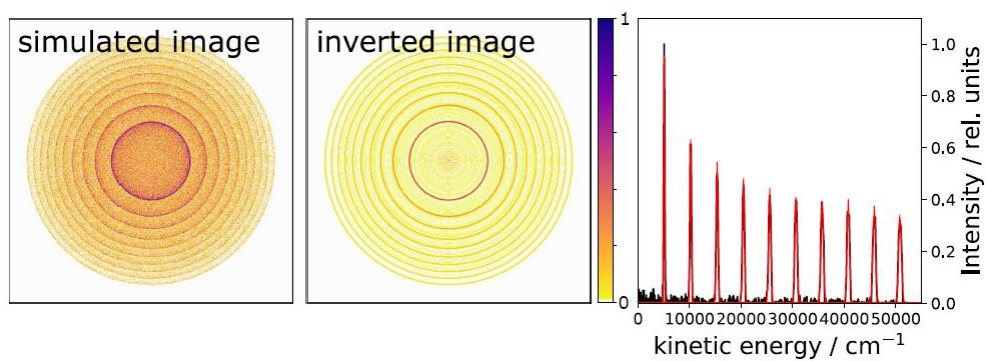


Figure S2. Left: Simulated velocity-map image of ten groups of electrons with kinetic energies ranging from 0.5 eV to 5.0 eV. Centre: Abel-inversion of the simulated image using the pBASEX [6] and the $l = 0$ Legendre polynomial. Right: Kinetic energy distributions of simulated electrons for a magnification factor, $N = 1$. The ten kinetic energy features are fitted with Gaussian functions (red line).

To determine the magnification factor, N , the kinetic energy axis is initially constructed using $N = 1$. The kinetic energy distribution of the simulated electrons (black line) and Abel-inverted image are shown in Figure S2. The ten features in the kinetic energy distribution are fitted with Gaussian functions (red line) to determine their width and central position.

According to Eppink and Parker [4], the radius of a feature in the velocity-map image and the particle velocity, v , is given by,

$$r = Nvt \quad (\text{S1})$$

$$v = \frac{r}{t} = Nv_{N=1} \quad (\text{S2})$$

Here, $v_{N=1}$ is the velocity assuming a homogeneous extraction field. The kinetic energy, $E_{\text{kin}} = mv^2/2$, extracted from the simulated velocity-map image, $E_{\text{kin,sim}}$, and the kinetic energy which is put into the simulation, $E_{\text{kin,input}}$, are then given by,

$$E_{\text{kin,input}} = N_{\text{ele}}^2 E_{\text{kin,sim}} \quad (\text{S1})$$

Figure S3 shows a plot of the electron kinetic energies retrieved from the simulation in Figure S2 as a function of the input kinetic energies of the simulated electrons.

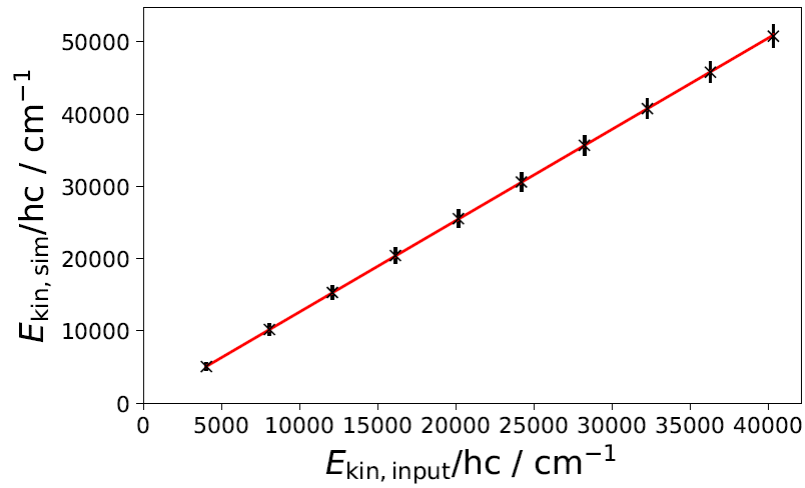


Figure S3. Relation between the kinetic energy extracted from the simulated velocity-map image, $E_{\text{kin,sim}}$, and kinetic energy of the simulated electrons, $E_{\text{kin,input}}$. The magnification factor of the velocity-map imaging spectrometer is determined from the slope of a linear fit to the data, which is $N_{\text{e}}^{-2} = 1.26 \pm 0.02$, according to Equation S3.

According to Equation S3, the square of the magnification factor, N_{e-}^2 , is retrieved as the slope of a linear fit to the data, and the magnification factor for velocity-map imaging of photoelectrons is therefore obtained as $N_{e-} = 1.12 \pm 0.01$.

The error bars in Figure S3 represent the full-width-at-half-maximum of Gaussian fits to the electron kinetic energy distribution. These can be used to estimate the energy resolution of the spectrometer which is 0.1 eV in the image centre and 0.4 eV at the detector edge.

B. Photoionization of vanadium atoms

To check the calibration of the newly-established electron imaging capabilities of our instrument, velocity-map images of photoelectrons from the (2+1)-REMPI ionization of vanadium atoms via the f^4F_J state were recorded. Figure S4 shows velocity-map images of photoelectrons recorded in vicinity of the $f^4F_J \leftarrow a^4F_J$ for $\Delta J = 0$ and $J'' = 3/2, 5/2, 7/2$, and $9/2$. The recorded velocity-map image is shown in the left-hand column, the Abel-inverted image is shown in the centre column and the retrieved kinetic energy distribution (black line) is shown in the right-hand side column. Velocity-map image data are analysed using the magnification factor determined for velocity-map imaging of electrons in the previous section. The ionization laser is polarized along the vertical axis, as indicated in Figure S4.

The electron kinetic energy distributions are compared to kinetic energies expected for a three-photon ionization of the V atom from the spin-orbit levels in the electronic ground state to the a^5F_{J+} and a^5D_{J+} states of the V^+ ion. The energies of the photoionization products, the photon energy, and the atom internal energy is given according to conservation of energy as:

$$E_{kin,ele} = E_V + 3h\nu - E_{V^+} - E_i \quad (S4)$$

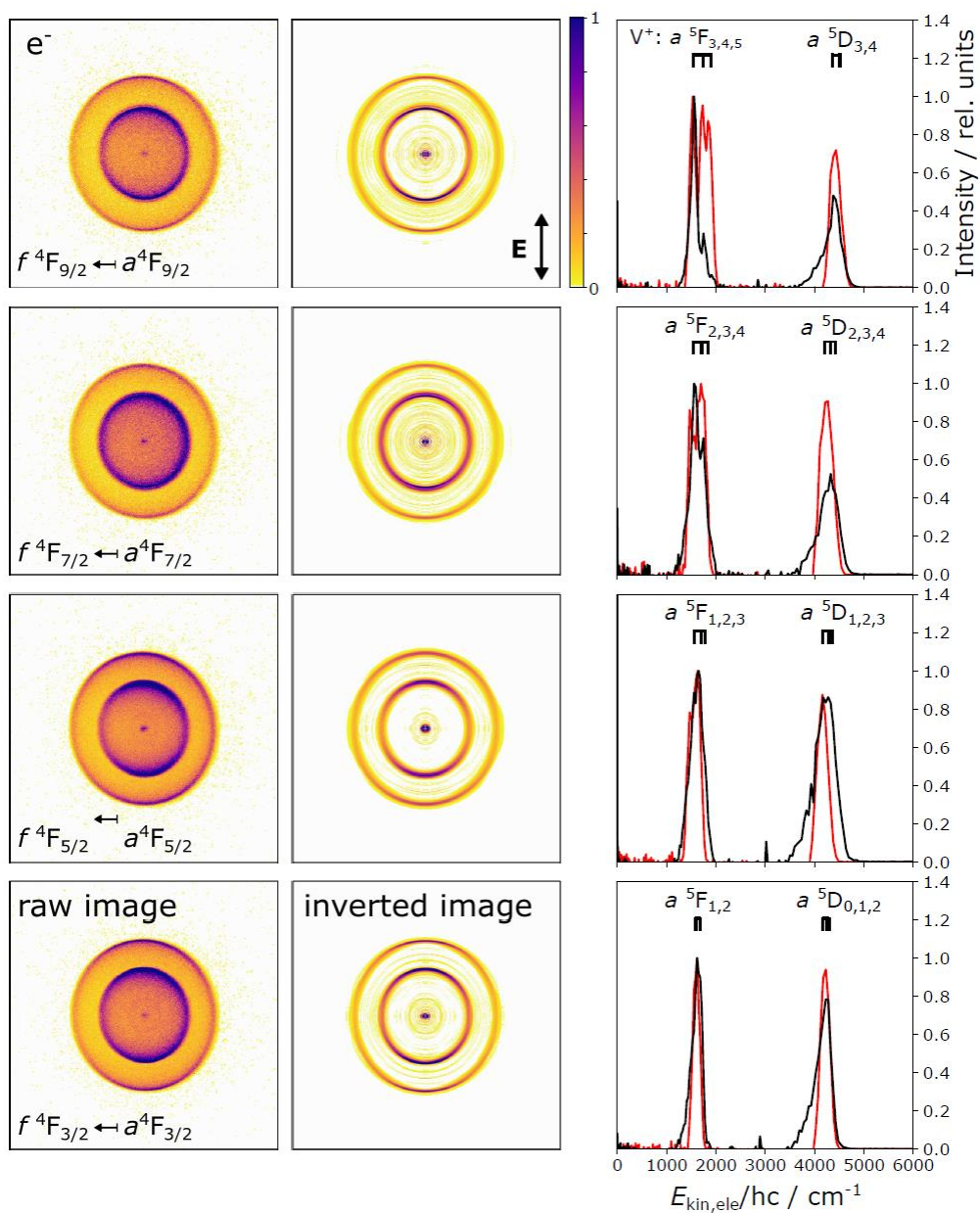


Figure S4. Photoelectron velocity-map images of the (2+1)-REMPI via the f^4F_J state for $J' = 3/2, 5/2, 7/2, 9/2$ from the top to bottom row. The recorded velocity-map image is shown in the left-hand side column, the inverted images in the central column, and the electron kinetic energy distribution is shown in the right-hand side column. The electron kinetic energy distributions (black line) are compared to simulated kinetic energies of photoelectrons for different accessible V^+ electronic states (red).

Here, E_i is the ionization energy which has been determined previously as 6.7461 eV (54411 cm^{-1}) [1]. The energies of the spin-orbit levels of the electron ground state $a^4F_{J''}$ in the vanadium atom and the energies of the a^5F_{J+} and a^5D_{J+} in the V^+ ion is given in Table S2.

J	$E_V(a^4F_{J''}) / \text{cm}^{-1}$	$E_{V^+}(a^5D_{J+}) / \text{cm}^{-1}$	$E_{V^+}(a^5F_{J+}) / \text{cm}^{-1}$
0	-	0.000	-
1	-	36.1017	2605.0400
3/2	0.000	-	-
2	-	106.6421	2687.2090
5/2	137.383	-	-
3	-	208.7901	2808.9590
7/2	323.432	-	-
4	-	339.1256	2968.3883
9/2	552.955	-	-
5	-	-	3162.9673

Table S2. Energy levels of the $a^4F_{J''}$ manifold for $J'' = 3/2; 5/2; 7/2$, and $9/2$ taken from Reference [2] and [3]. Energy levels of the a^5D_J and a^5F_J manifold for $J = 0, 1, 2, 3, 4$, and 5 taken from Reference [7].

Using Equation S4, the electron kinetic energies are derived for the accessible spin-orbit levels and electronic states of the V^+ ion, and the electron kinetic energies are compared to the velocity-map imaging results in Figure S4. The experimental determined electron kinetic energy (black line) is compared to kinetic energies retrieved from a simulation of the velocity-map image using the derived kinetic energies employing the SIMION software package [5] (red line). The simulated and experimental kinetic energy distribution are in very good agreement and illustrate that VMI studies of photoelectrons can be performed with our experimental set-up. The width of the features in the experimental data and the simulated kinetic energy distributions is similar, which indicates that the kinetic energy resolution is mainly limited by the kinetic energy resolution of the VMI spectrometer.

SIII. References

- [1]A. M. James, P. Kowalczyk, E. Langlois, M. D. Campbell, A. Ogawa, and B. Simard, *J Chem Phys* **101** (6), 4485 (1994).
- [2]E. B. Saloman and A. Kramida, *Astrophys J Suppl S* **231** (2) (2017).
- [3]E. B. Saloman and A. Kramida, *Astrophys J Suppl S* **240** (2) (2019).
- [4]A. T. J. B. Eppink and D. H. Parker, *Rev Sci Instrum* **68** (9), 3477 (1997).
- [5]D. J. Manura and D.D. Dahl, SIMION v8.1 (2013).
- [6]G. A. Garcia, L. Nahon, and I. Powis, *Rev Sci Instrum* **75** (11), 4989 (2004).
- [7]E. B. Saloman and A. Kramida, *Astrophys J Suppl S* **231** (2) (2017).